J|A|C|S ARTICLES

Published on Web 12/02/2010

Discriminative Response of Surface-Confined Metalloporphyrin Molecules to Carbon and Nitrogen Monoxide

Knud Seufert,* Willi Auwärter,* and Johannes V. Barth

Physik Department E20, Technische Universität München, D-85748 Garching, Germany

Received June 23, 2010; E-mail: Knud.Seufert@ph.tum.de; Wilhelm.Auwaerter@ph.tum.de

Abstract: The binding of small gas molecules to metalloporphyrins is of both fundamental scientific and technological interest. It plays a key role in the transport of respiratory gases, catalytic processes in biological systems, and artificial nanostructures for sensing. Here, we present a detailed molecular-level investigation regarding the interaction of nitrogen monoxide (NO) and carbon monoxide (CO) with metallo-tetraphenylporphyrin (M−TPP, M = Co, Fe) arrays, anchored on a noble metal Ag(111) surface, providing M−TPP species with a distinct saddle-shape conformation. Scanning tunneling microscopy and spectroscopy experiments reveal that the impact of CO and NO is strikingly different on both species. In the case of CO, the M−TPP core can be dressed by either one or two carbon monoxide ligands, whereby the porphyrin geometric and electronic structure remains nearly unaffected. In contrast, following NO exposure exclusively a mononitrosyl species evolves. The NO axial ligation induces a relaxation of the adsorption-induced molecular deformation and markedly modifies the electronic structure of the porphyrin.

Introduction

Because of their inherent functionality, porphyrin molecules play a key role in numerous biological and technical processes like oxygen transport in blood, photosynthesis, catalytic conversions mediated by cytochrome, charge transfer in photovoltaic elements, or chemical sensing.[1−4] Hereby, special focus lies on the metal centers with 4-fold coordination by the tetrapyrrole macrocycle, as they form the active site for attachment of axial ligands. For example, the Fe center in heme reversibly binds small gas molecules during respiratory action, or the Co center in vitamin B12 mediates in exchange processes of methyl. Herein, beyond the nature of the metal center and the meso substituents, the macrocycle conformation represents a crucial factor to regulate the metalloporphyrin's functional properties.[5] Accordingly, the interaction of axial ligands with metalloporphyrins has been extensively studied in the gas phase, solution, and solid state. However, an understanding of the response of surface-anchored porphyrins toward small molecules is currently just emerging.[6−13] This is surprising for two reasons: first, for many possible technical applications the functional porphyrin species have to be anchored on a support and, second, the adsorption of the porphyrin can drastically modify its physicochemical properties.[14] The surface bonding thus needs to be fully considered to rationalize the geometric and electronic properties of the functional molecular unit. For example, the catalytic activity of surface-supported Co−TPP films drastically differs from their gas-phase counterparts,[15,16] or the magnetic characteristics of iron porphyrins can be determined by an appropriate substrate.[17,18] Furthermore, the overall conformation of meso-substituted phenyl or pyridyl species is influenced by the surface anchoring generally leading to a distinct saddle shape.[19−24] Consequently, adsorbed metalloporphyrin species represent model systems for surface-confined coordination

(1) Meunier, B. *Chem. Rev.* **1992**, *92*, 1411–1456.
(2) Wasielewski, M. R. *Chem. Rev.* **1992**, *92*, 435–461.
(3) Milgrom, L. R. *The Colors of Life*; Oxford University Press: New York, 1997.
(4) Kadish, K. M. S. K. M., Guilard, R. *The Handbook of porphyrins*; Academic Press: New York, 1999.
(5) Shelnutt, J. A.; Song, X. Z.; Ma, J. G.; Jia, S. L.; Jentzen, W.; Medforth, C. J. *Chem. Soc. Rev.* **1998**, *27*, 31–41.
(6) Collman, J. P.; Brauman, J. I.; Halbert, T. R.; Suslick, K. S. *Proc. Natl. Acad. Sci. U.S.A.* **1976**, *73*, 3333–3337.
(7) Maxwell, J. C.; Caughey, W. S. *Biochemistry* **1976**, *15*, 388–396.
(8) Shaanan, B. *J. Mol. Biol.* **1983**, *171*, 31–59.
(9) Williams, F. J.; Vaughan, O. P. H.; Knox, K. J.; Bampos, N.; Lambert, R. M. *Chem. Commun.* **2004**, 1688–1689.
(10) Hulsken, B.; Van Hameren, R.; Gerritsen, J. W.; Khoury, T.; Thordarson, P.; Crossley, M. J.; Rowan, A. E.; Nolte, R. J. M.; Elemans, J.; Speller, S. *Nat. Nanotechnol.* **2007**, *2*, 285–289.
(11) Flechtner, K.; Kretschmann, A.; Steinrück, H. P.; Gottfried, J. M. *J. Am. Chem. Soc.* **2007**, *129*, 12110–12111.
(12) Domke, K. F.; Pettinger, B. *ChemPhysChem* **2009**, *10*, 1794–1798.
(13) Wäckerlin, C.; Chylarecka, D.; Kleibert, A.; Müller, K.; Iacovita, C.; Nolting, F.; Jung, T. A.; Ballav, N. *Nat. Commun.* **2010**, *1*, 61.
(14) Visser, J.; Katsonis, N.; Vicario, J.; Feringa, B. L. *Langmuir* **2009**, *25*, 5980–5985.
(15) Mochida, I.; Tsuji, K.; Suetsugu, K.; Fujitsu, H.; Takeshita, K. *J. Phys. Chem.* **1980**, *84*, 3159–3162.
(16) Berner, S.; Biela, S.; Ledung, G.; Gogoll, A.; Backvall, J. E.; Puglia, C.; Oscarsson, S. *J. Catal.* **2006**, *244*, 86–91.
(17) Scheybal, A.; Ramsvik, T.; Bertschinger, R.; Putero, M.; Nolting, F.; Jung, T. A. *Chem. Phys. Lett.* **2005**, *411*, 214–220.
(18) Wende, H. et al. *Nat. Mater.* **2007**, *6*, 516–520.
(19) Yokoyama, T.; Yokoyama, S.; Kamikado, T.; Mashiko, S. *J. Chem. Phys.* **2001**, *115*, 3814–3818.
(20) Auwärter, W.; Weber-Bargioni, A.; Riemann, A.; Schiffrin, A.; Gröning, O.; Fasel, R.; Barth, J. V. *J. Chem. Phys.* **2006**, *124*, 194708.
(21) Auwärter, W.; Klappenberger, F.; Weber-Bargioni, A.; Schiffrin, A.; Strunskus, T.; Woll, C.; Pennec, Y.; Riemann, A.; Barth, J. V. *J. Am. Chem. Soc.* **2007**, *129*, 11279–11285.
(22) Klappenberger, F.; Weber-Bargioni, A.; Auwärter, W.; Marschall, M.; Schiffrin, A.; Barth, J. V. *J. Chem. Phys.* **2008**, *129*, 10.
(23) Weber-Bargioni, A.; Auwärter, W.; Klappenberger, F.; Reichert, J.; Lefrancois, S.; Strunskus, T.; Woll, C.; Schiffrin, A.; Pennec, Y.; Barth, J. V. *ChemPhysChem* **2008**, *9*, 89–94.

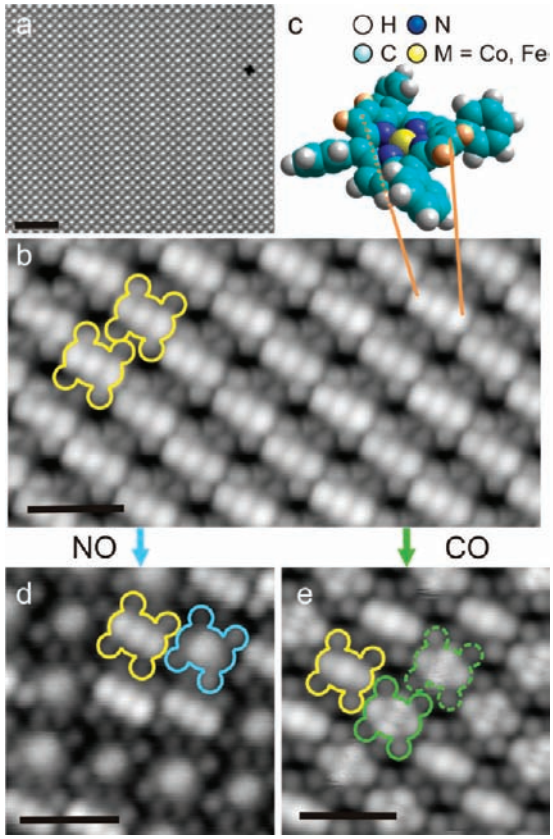

Figure 1. STM topography of a Co−TPP array on Ag(111) and its response toward exposure of NO and CO. (a) Overview of a large well-ordered array of bare Co−TPP. (b) Submolecular resolution of bare Co−TPP. Two Co−TPPs are outlined in yellow to facilitate identification of the molecular moieties. (c) Saddle-shape conformational adaptation of Co−TPP. In the model, pyrrole hydrogens pointing away from the surface are emphasized in orange. (d) Co−TPP array after a dosage of NO at 150 K. The yellow frame marks a bare Co−TPP, and the blue frame highlights a NO-ligated Co−TPP module. (e) Co−TPP array after dosing small amounts of CO at ∼10 K. Again, the yellow frame represents a bare Co−TPP, whereas two different green frames, with solid and dashed lines, respectively, show two different CO decorated species (image parameters: (a) $U = -482$ mV, $I =$ 0.1 nA, scale bar = 100 Å, (b) $U = -0.666$ V, $I = 0.11$ nA, scale bar = 20 Å, (d) $U = -0.7$ V, $I = 55$ pA, scale bar = 20 Å, (e) $U = -0.59$ V, $I = 30$ pA, scale bar = 20 Å).

chemistry, providing a well-defined environment for metal centers in proximity to both macrocycle and substrate atoms.[25−27]

Here we present a first comparative experimental report addressing the interaction between diatomic gas molecules and surface-anchored metalloporphyrins on the single-molecule level. To this end, we focus on two archetypical metalloporphyrins, namely, Co−tetraphenylporphyrin (Co−TPP) and Fe−tetraphenylporphyrin (Fe−TPP). These species are composed of a macrocycle hosting a metal center M (M = Co, Fe) and four phenyl rings as meso substituents (cf. structural model in Figure 1c). In recent years, much effort was focused on the controlled assembly of highly ordered, two-dimensional layers from such M−TPP units.[28] In particular, the formation and ordering of porphyrin arrays on Ag(111) as well as the electronic structure and geometric conformation of their constituting M−TPP modules are well characterized by previous studies.[24,29−32] Accordingly, they serve as perfect templates to study the effects of gas adsorption. In our experiments we compare carbon monoxide (CO), a toxic gas interfering with the oxygen delivery to bodily tissues, and nitrogen monoxide (NO), a highly relevant biomolecule,[33,34] as ligands. NO and CO are also formed in combustion and occur as reaction intermediates in catalytic processes.

Scanning tunneling microscopy (STM) allows us to visualize the effects of these small gas molecules on metalloporphyrins with submolecular resolution. Moreover, the electronic structure of the surface-anchored porphyrin upon attachment of the NO or CO ligand is analyzed in unprecedented detail by spatially resolved scanning tunneling spectroscopy (STS).

Experimental Section

All experiments were performed in a commercial low-temperature scanning tunneling microscope (LT-STM) based on the design described in ref 35, produced by SPS-Createc and mounted in a custom-designed ultrahigh vacuum (UHV) setup.[36] The system base pressure was below 2×10^{-10} mbar, and all measurements were performed at 6 K to obtain high-resolution topographic and spectroscopic data. In all figure captions U refers to the bias voltage applied to the sample. The STM images were taken in constant current mode, whereas a lock-in technique was used to record the spectroscopic dI/dU data (spectra 969 Hz, $\Delta U = 25$ mV; maps 2969 Hz, $\Delta U = 25$ mV). The STM images are handled by the WsXM program (www.nanotec.es). The etched tungsten tip is prepared by argon bombardment and controlled dipping into the bare surface. The Ag(111) single-crystal surface was cleaned by repeated cycles of argon sputtering (800 eV ion energy and ∼10 μA sputter current) and annealing to 725 K. Subsequently, Co−TPP was deposited by organic molecular beam epitaxy (OMBE) from a quartz crucible held at 625 K with a rate below one monolayer per hour, (ML)/h. The Co−TPP molecules were synthesized by the Ruben group at INT Karlsruhe and degassed carefully, resulting in a background pressure in the 10^{-10} mbar range during evaporation. The Fe−TPP species was synthesized in situ by exposing a 2H−TPP layer to an atomic beam of Fe (purity 99.998%). This procedure, which allows us to fabricate clean Fe−TPP arrays, is described in detail in refs 29 and 32. After deposition of the porphyrin molecules at room temperature, the sample was cooled to 150 K for dosing of nitrogen monoxide (specified purity 99.8%) and subsequently transferred into the STM. We used both a low temperature and a low NO dose to avoid rearrangement of the molecules inside of the islands as reported in ref 37. The same

(24) Auwärter, W.; Seufert, K.; Klappenberger, F.; Reichert, J.; Weber-Bargioni, A.; Verdini, A.; Cvetko, D.; Dell'Angela, M.; Floreano, L.; Cossaro, A.; Bavdek, G.; Morgante, A.; Seitsonen, A. P.; Barth, J. V. *Phys. Rev. B* **2010**, *81*, 245403.
(25) Barth, J. V. *Surf. Sci.* **2009**, *603*, 1533–1541.
(26) Gottfried, J. M.; Marbach, H. *Z. Phys. Chem., Int. J. Res. Phys. Chem. Chem. Phys.* **2009**, *223*, 53–74.
(27) Lin, N.; Stepanow, S.; Ruben, M.; Barth, J. V. *Top. Curr. Chem.* **2009**, *287*, p 1–44.
(28) Scudiero, L.; Barlow, D. E.; Hipps, K. W. *J. Phys. Chem. B* **2000**, *104*, 11899–11905.
(29) Auwärter, W.; Weber-Bargioni, A.; Brink, S.; Riemann, A.; Schiffrin, A.; Ruben, M.; Barth, J. V. *ChemPhysChem* **2007**, *8*, 250–254.
(30) Lukasczyk, T.; Flechtner, K.; Merte, L. R.; Jux, N.; Maier, F.; Gottfried, J. M.; Steinrück, H. P. *J. Phys. Chem. C* **2007**, *111*, 3090–3098.
(31) Zotti, L. A.; Teobaldi, G.; Hofer, W. A.; Auwärter, W.; Weber-Bargioni, A.; Barth, J. V. *Surf. Sci.* **2007**, *601*, 2409–2414.
(32) Buchner, F.; Flechtner, K.; Bai, Y.; Zillner, E.; Kellner, I.; Steinrück, H. P.; Marbach, H.; Gottfried, J. M. *J. Phys. Chem. C* **2008**, *112*, 15458–15465.
(33) Culotta, E.; Koshland, D. E. *Science* **1992**, *258*, 1862–1865.
(34) Archer, S. *FASEB J.* **1993**, *7*, 349–360.
(35) Meyer, G. *Rev. Sci. Instrum.* **1996**, *67*, 2960–2965.
(36) Auwärter, W.; Schiffrin, A.; Weber-Bargioni, A.; Pennec, Y.; Riemann, A.; Barth, J. V. *Int. J. Nanotechnol.* **2008**, *5*, 1171–1193.
(37) Buchner, F.; Seufert, K.; Auwärter, W.; Heim, D.; Barth, J. V.; Flechtner, K.; Gottfried, J. M.; Steinrück, H. P.; Marbach, H. *ACS Nano* **2009**, *3*, 1789–1794.

results can be reached by exposure of the porphyrins to NO at about 10 K. Due to a low sticking probability of carbon monoxide on the metalloporphyrins at temperatures exceeding ~120 K, we exposed the sample to CO (specified purity 99.97%) in situ (directly in the measurement position inside the cooling shields of the STM) at temperatures between 6 and 20 K.

In the presented experiments, we typically applied submonolayer coverages of the porphyrins and also kept the NO or CO occupation clearly below the saturation values. This procedure results in clean metal patches, bare porphyrins, and decorated porphyrins on the same surface and allows us to take measurements on all species with the very same STM tip under identical conditions. However, full monolayer coverage of porphyrins as well as its complete saturation by the CO or NO ligands can be achieved without difficulty.

Results and Discussion

On the Ag(111) surface, Co−TPP forms large highly ordered arrays (see Figure 1a). The submolecular resolution image (Figure 1b) shows an ant-like protrusion, which defines the main axis of the molecule.[24,38] The metal ion is visible in the center, and the two additional features represent one opposing pair of upward-tilted pyrrol rings, while the other pair is tilted downward. This appearance emerges due to a saddle-shape deformation of the porphyrin macrocycle, highlighted in Figure 1c, as comprehensively described in ref 23. The additional dim protrusions correspond to the four phenyl legs per molecule. Details of the geometric and electronic structure of Co−TPP on Ag(111) can be found in ref 24.

Topographic Appearance of Nitrogen Monoxide vs Carbon Monoxide Ligated Co−TPP. After dosing small amounts of nitrogen monoxide (NO) at 150 K, some of the molecules in the Co−TPP array show a markedly modified appearance (Figure 1d). The previous 2-fold symmetry of the molecular core is lifted, and only one round central protrusion is dominating the molecular contrast. This new species is assigned to the influence of the NO, as the percentage of modified molecules scales with the NO dose. The appearance of NO/Co−TPP in STM images depends drastically on the chemical termination of the STM tip (see Figure S1 in the Supporting Information). Besides the imaging mode exhibiting a broad central protrusion visible in Figure 1d that is induced by a NO termination of the tip, the NO/Co−TPP species appears with a central depression, showing a close resemblance to metal-free 2H−TPP (see Figure 5), if a bare metal tip is used. Similar effects are known from imaging small molecules[39] on metal surfaces and do not affect the conclusions drawn in the following. The imaging mode with a central depression was also reported for different metalloporphyrins and ligated phthalocyanines.[40,41] Modification of the porphyrin core by NO attachment indicates that a single nitrogen monoxide ligand coordinates to the Co center, in agreement with expectations from 3D systems[42] and recent observations from space-integrating photoelectron spectroscopy experiments.[11,26] In addition, the former saddle-shape distortion of the bare Co−TPP seems to be reduced upon NO coordination as the pronounced symmetry break expressed in the main axis described above disappeared for NO/Co−TPP (vide infra).

The STM data yield no direct indication for a tilting or bending of the NO away from the surface normal, which is emphasized in most earlier reports.[43] One possibility to reconcile our observations with the model proposed in the literature[44] is to assume that the NO is indeed tilted but spinning rapidly around the metal center. In this case our measuring technique cannot resolve the actual NO position but only maps a temporal average. Such a spinning or even tilting motion may be also tip induced. Indeed, calculations predict a considerable flexibility of the M−NO unit, even allowing a 180° bond angle without drastic energy cost.[42] Furthermore, an electronic transparency of the NO in the STM imaging process could explain the appearance of the relaxed molecule as described above.

Exposure of Co−TPP arrays to carbon monoxide results in two new species, both markedly different from NO/Co−TPP (Figure 1e). The main axis of the Co−TTP is still clearly visible and remains unaffected, but two new protrusions located on the secondary axis (i.e., perpendicular to the main axis) of the molecule emerge, resulting in a cross-like appearance of the molecule. These additional features apparently originate from the carbon monoxide attachment. A closer look at Figure 1e reveals that two related cross-like structures can be discriminated. The first species (solid green frame) shows five stable protrusions whereof three correspond to the ant-like, bare Co−TPP features and the two extra protrusions reflect CO decoration. This species is called static cross. The second one (dashed green frame) exhibits again the three protrusions of the Co−TPP main axis. However, the two additional CO-induced features are frizzy and appear noisy, indicating movements at a frequency exceeding the scanning frequency of the STM. This species is designated labile cross. Before addressing the bonding of CO to the Co−TPP, including the impact on the electronic structure of the molecule, we first clarify the nature of the two cross-like species by an STM manipulation experiment.

For the lateral manipulation procedure the STM tip is used as a tool to translate adsorbates across a surface, as successfully demonstrated for single atoms[45] or CO molecules[46] on metal substrates. Here, we stabilized the tip at 500 mV and 30 pA above a static cross (see Figure 2a and 2d) and approached the surface by increasing the tunneling current to 1 nA. Subsequently, the tip was laterally moved to a neighboring Co−TPP molecule and finally retracted to its initial height. The following STM image shows that this procedure splits one static cross into two labile ones (Figure 2b and 2e). Applying the same manipulation sequence again, it is possible to reunite the two labile species again to the previous configuration, however now localized on the neighboring molecule (Figure 2c and 2f). Consequently, the static cross is composed of two CO molecules attached to one Co−TPP, whereas the labile cross represents a single CO molecule attached to Co−TPP.

The double protrusion associated with the CO binding is located above the pyrrole rings and aligned with the secondary axis of the Co−TPP. Accordingly, the CO occupies distinct, symmetric positions at the porphyrin core. With only one CO

(38) Comanici, K.; Buchner, F.; Flechtner, K.; Lukasczyk, T.; Gottfried, J. M.; Steinrück, H. P.; Marbach, H. *Langmuir* **2008**, *24*, 1897–1901.
(39) Bartels, L.; Meyer, G.; Rieder, K. H. *Appl. Phys. Lett.* **1997**, *71*, 213–215.
(40) Barlow, D. E.; Hipps, K. W. *J. Phys. Chem. B* **2000**, *104*, 5993–6000.
(41) Takami, T.; Clark, A.; Caldwell, R.; Mazur, U.; Hipps, K. W. *Langmuir* **2010**, *26*, 12709–12715.
(42) Ghosh, A. *Acc. Chem. Res.* **2005**, *38*, 943–954.
(43) Westcott, B. L.; Enemark, J. H. *Transition metal nitrosyls*; John Wiley & Sons Inc.: New York, 1999.
(44) Enemark, J. H.; Feltham, R. D. *Coord. Chem. Rev.* **1974**, *13*, 339–406.
(45) Eigler, D. M.; Schweizer, E. K. *Nature* **1990**, *344*, 524–526.
(46) Meyer, G.; Neu, B.; Rieder, K. H. *Appl. Phys. A: Mater. Sci. Process.* **1995**, *60*, 343–345.

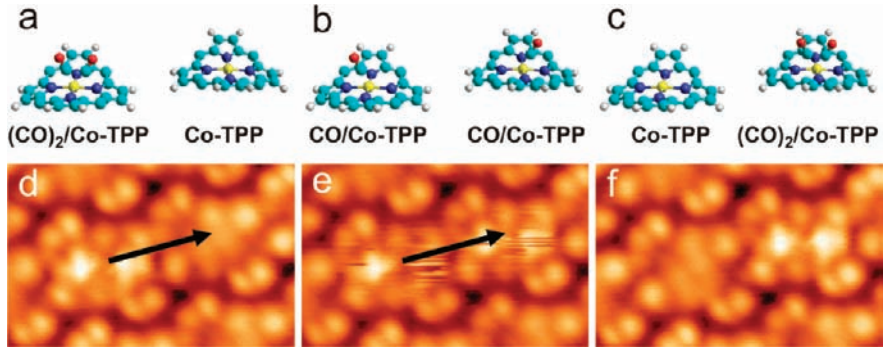

Figure 2. (a−c) Schematic models of two metalloporphyrins and two CO ligands illustrating the experimental situations in d−f (phenyl legs not shown for clarity). (d−f) Transfer of CO ligands between Co−TPP molecules by single-molecule manipulation steps. The black arrows indicate the path of the STM tip for CO transfer. STM data are recorded at 500 mV sample bias.

attached to the porphyrin, this ligand is rapidly flipping between the two positions. As the corresponding time scale is much shorter than that for STM imaging, we observe the appearance of a labile cross. This indicates that the energy barrier the CO has to overcome between the two equilibrium positions is rather low. However, effects of the proximity of the STM tip on the flipping cannot be excluded. The controlled lateral manipulation of the CO on Co−TPP islands is possible over large distances (exceeding 100 Å) and in different directions (not only following the main symmetry directions of the array).

There are two possibilities for the unusual carbonyl binding to the Co−TPP molecules consistent with the presented experimental observations: One or two CO molecules might coordinate to the metal center via the carbon with their axis symmetrically tilted away from the surface normal. This interpretation would be in line with the coordination of one or two CO molecules to individual Fe adatoms on Ag(110),[47] however inconsistent with the generally expected monocarbonyl ligation at porphyrins with late transition metal centers.[44] The second possibility is a binding of the polar CO to the macrocycle of the porphyrin, either by coupling to the π system of the underlying pyrrole rings as described in ref 48 or by interaction with the pyrrolic N atoms. A detailed account of the unusual carbonyl ligation scenario will be presented elsewhere. The two key messages of the experiments presented in this paragraph are the direct proof, on a single-molecule level, that either one or two COs can be weakly attached to a surface-anchored Co−TPP molecule and the different adsorption characteristics of carbon monoxide and nitrogen monoxide ligands.

Electronic Structure of Nitrogen Monoxide vs Carbon Monoxide Ligated Co−TPP. To check the influence of NO on the electronic structure of Co−TPP, we recorded d*I*/d*U* spectra at different locations on a bare Co−TPP molecule and on NO/Co−TPP (see Figure 3). Because of the limited stability of the nitrosyl species, where the NO ligand is abstracted at high tunneling voltages, we focused on the "low-energy" region with bias voltages in the range from −700 to +500 mV. The curves in Figure 3e represent three spectra recorded on different parts of a single bare Co−TPP. Whereas the spectra taken above the Co center (light yellow) and the pyrrole ring of the second axis (yellowish brown) show no prominent features, a pronounced peak at a bias voltage of approximately −600 mV is detected above the pyrrole of the main axis (bright yellow). This feature was assigned to the highest occupied molecular orbital (HOMO)

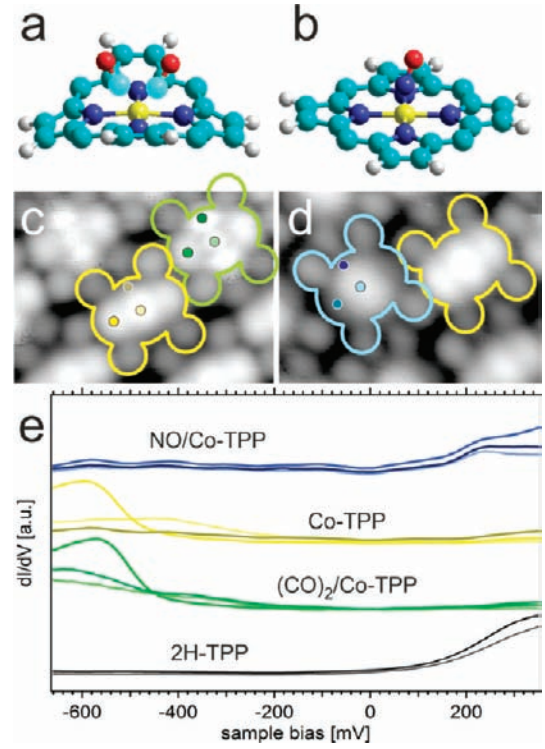

Figure 3. Tunneling spectroscopy data revealing the differences of pristine vs NO and CO ligated Co−TPP species. (a) Schematic model of $(CO)_2$/Co−TPP (*meso*-phenyl groups omitted for clarity). (b) Schematic model of NO/Co−TPP (*meso*-phenyl groups omitted for clarity). (c) Topographic image of Co−TPP after the dosing of CO. Bare Co−TPP is outlined in yellow and $(CO)_2$/Co−TPP in green. The colored dots represent the positions of d*I*/d*U* spectra. (d) Topographic image of Co−TPP after exposure to NO. Bare Co−TPP is outlined in yellow and NO/Co−TPP in blue. The colored dots represent the positions of d*I*/d*U* spectra. (e) d*I*/d*U* spectra of three different species at the three indicated different locations of the molecule. For comparison, reference spectra of 2H−TPP (spectra at same different positions, two of which cannot be discriminated) are added. Spectra on different species are vertically offset for clarity.

of Co−TPP/Ag(111) with weight on the porphyrin macrocycle including contributions from Co electronic states (for a detailed discussion see ref 24).

The spectra on NO/Co−TPP, taken at identical positions with the very same STM tip, reveal significant changes (blue curves, Figure 3e). We observe an increased density of states above the Fermi level, and more importantly, the pronounced HOMO peak dominant for bare Co−TPP is completely expunged. In strong contrast to the NO case, attachment of either one or two CO ligands to the Co−TPP entails only a marginal change in

(47) Lee, H. J.; Ho, W. *Science* **1999**, *286*, 1719–1722.
(48) Gallivan, J. P.; Dougherty, D. A. *Org. Lett.* **1999**, *1*, 103–105.

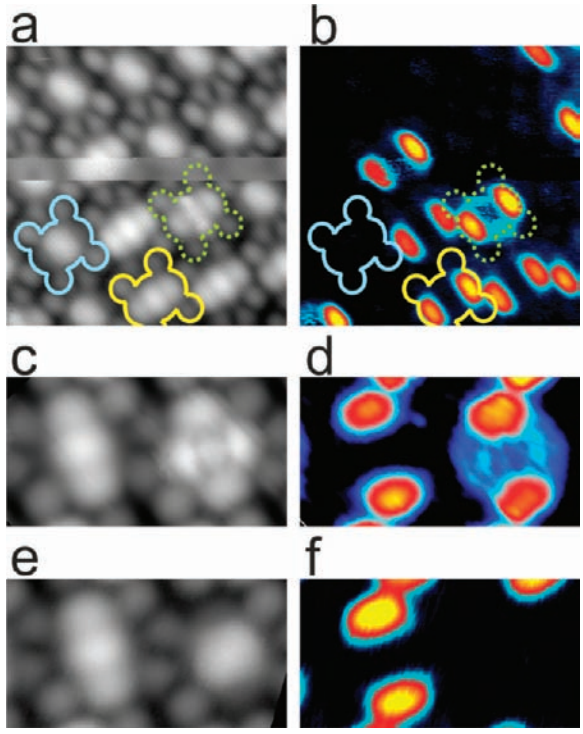

Figure 4. Topographic (a) and spectroscopic (b) data of a mixed array including bare Co−TPP (yellow frames), CO/Co−TPP (dashed green frames), and NO/Co−TPP (blue frames). The dI/dU map presented in b reveals the spatial electron density distribution of the Co−TPP HOMO for all three species (image parameters: $U = -600$ mV; $I = 55$ pA; size is 55.4 Å × 55.4 Å). (c and e) Closer topographic look to a bare Co−TPP compared to a $(CO)_2$/Co−TPP and NO/Co-TPP. (d and f) Corresponding dI/dU maps at the energy of the molecular HOMO.

the electronic structure of the molecule (see green curves in Figure 3e). The molecular HOMO is still at the same energetic position, and no significant additional features emerge.

Further insight is gained by analyzing the spatial electron density distribution of the HOMO state, which can be directly visualized by tunneling spectroscopy mapping. Figure 4a and 4b presents data of a mixed Co−TPP, NO/Co−TPP, and CO/Co−TPP array. The dI/dU maps taken −600 mV reproduced in Figure 4b, 4d, and 4f show that the characteristic two-lobe contrast only exists for bare Co−TPP (yellow frame) and CO/Co−TPP (green dotted frame) but not for the NO/Co−TPP species (blue frame). The latter appear transparent at this energy. Together with the similarity between STS spectra of 2H−TPP and NO/Co−TPP and the close resemblance of topographic images of these two species taken with a metallic tip, this finding has two interrelated implications: (i) the bonding of NO to the Co center involves the same Co electronic states, which couple the Co to the porphyrin macrocycle. Thus, the NO coordination partially affects the Co−macrocycle interactions, and the NO/Co−TPP is imaged similar as the metal-free 2H−TPP counterpart. (ii) The pronounced saddle-shape distortion of the Co−TPP macrocycle is reduced upon NO coordination. Both effects point to a reduced molecule−substrate interaction as a consequence of the attachment of NO axial ligand. This conclusion agrees with the interpretation of space-averaging photoemission data on NO/Co−TPP.[11] There, the vanishing of the spectral feature 600 meV below the Fermi level, corresponding to the HOMO signature, was tentatively explained by a weakening of the Co−Ag bond induced by the NO ligand.

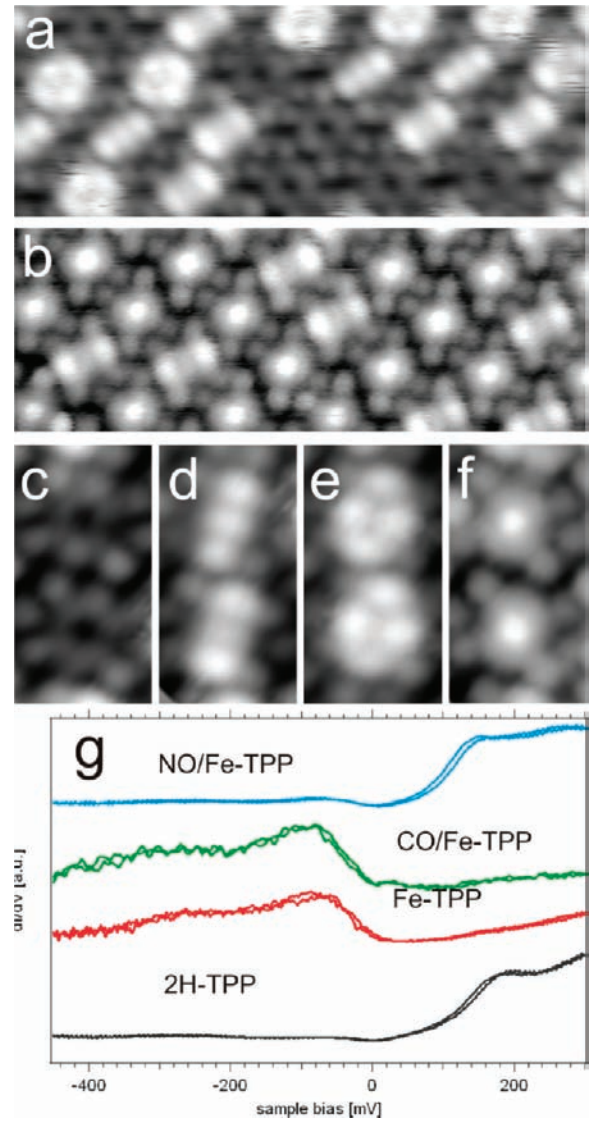

Figure 5. (a) Overview topographic image of a mixed array of 2H−TPP, Fe−TPP, and $(CO)_{1,2}$/Fe−TPP following exposure to CO. (b) Mixture of Fe−TPP and NO/Fe−TPP. (c) High-resolution STM topograph of two 2H−TPP molecules on Ag(111). (d) In-situ metalated Fe−TPP. (e) CO attached to Fe−TPP. (f) NO attached to Fe−TPP. (g) Corresponding dI/dU spectra of images c−f. The spectra are averaged over different positions of the molecule and vertically offset for clarity (image parameters: (a, c−e) $U = -240$ mV, $I = 35$ pA; (b and f) $U = -600$ mV, $I = 100$ pA; size of a and b, 150 Å × 55.6 Å; size of c−f, 16.7 Å × 31.4 Å).

The dI/dU signature of the CO-decorated Co−TPP depicted in Figure 4b and 4d corroborates the conclusions drawn from the point spectra: Compared to bare Co−TPP, CO/Co−TPP and $(CO)_2$/Co−TPP only exhibit small additional intensity, distributed around the secondary molecular axis. This observation proves that the cross-like structure observed in the topographic STM images of $(CO)_2$/Co−TPP does not represent a nearly 4-fold symmetric macrocycle induced by a conformational relaxation of the saddle-shape distortion, but rather emerges from contributions of the CO ligands. The 2-fold symmetry given by the Co−TPP main axis persists, reflecting a weak interaction between the CO and the Co center. The Co−porphyrin bonds and the molecule−substrate interplay are hardly influenced, in striking contrast to the NO case. In view of the high affinity of CO to the metal centers in the 2+ oxidation state in metal-

loporphyrins as evidenced for example in heme, the weak CO−Co−TPP bond strength and the modest impact of the carbonyl ligation on the low-energy electronic structure of Co−TPP is somewhat surprising. It could either reflect a modified oxidation state of the Co center due to charge exchange with the underlying metal surface[30] resulting in a weaker interaction or point to an unusual adsorption configuration, where the COs are not exclusively bound to the Co center. However, the data reported in ref 49 indicate that no CO coordination to Co−TPP exists at room temperature for thick Co−TPP films, where the Co center is definitely in its original 2+ oxidation state.[11,24]

Response of Adsorbed Fe−TPP to Exposure of CO and NO. Motivated by the functional properties of Fe−porphyrin species in many biological systems, we extended our study to Fe−TPP molecules. In a first step, we synthesized Fe−TPP molecules directly on the Ag(111) surface under UHV conditions (see experimental part and ref 29). Due to the high reactivity of Fe−TPP at ambient conditions, this procedure is advantageous to obtain clean Fe−TPP arrays. In a second step, the Fe−TPP arrays are exposed to CO or NO to probe the bonding of adducts. Hereby, we followed the very same experimental protocols as in the Co−TPP case.

The detailed data shown in Figure 5c and 5d illustrate the synthesis steps: The exposure of free base 2H−TPP (Figure 5c) to a beam of Fe atoms results in a mixed layer of 2H−TPP and in-situ-metalated Fe−TPP where the two hydrogen atoms are replaced by an iron center. The Fe−TPP (Figure 5d) is characterized by an ant-like appearance, resulting from a saddle-shape distortion of the macrocycle, analogous to the Co−TPP case (compare Figure 1c). Again, an additional electronic state caused by the metalation is observable. These high-resolution images are consistent with reports on Fe−TPyP.[29] The subsequent in situ dosage of CO results, as described beforehand for Co−TPP, in cross-like structures with two extra protrusions perpendicular to the main axis of the molecule, whereby the former structure is essentially untouched (Figure 5e). Both static and labile crosses, equipollent to CO/Fe−TPP and $(CO)_2$/Fe−TPP, are observed. In contrast, NO changes both the topographic appearance and the low-energy electronic structure. Similar to the Co−TPP case, the molecular center appears round (Figure 5f) and the metal-related HOMO state is completely quenched. The gray curves in Figure 5g represent reference spectra of 2H−TPP. The red spectra, taken on Fe−TPP, exhibit an additional state at about −80 mV identified as the molecular HOMO, related to the metalation. CO attachment does not modify the low-energy electronic structure (green spectra). Upon NO exposure, the pronounced HOMO peak is quenched (blue spectra) and the electronic structure becomes comparable to the one of 2H−TPP. These experiments evidence a very similar impact of the employed diatomic gas molecules on surface-anchored Fe−TPP and Co−TPP.

(49) Kurtikyan, T. S.; Martirosyan, G. G.; Akopyan, M. E. *Kinet. Catal.* **2001**, *42*, 281–288.

Conclusion

We presented a comprehensive molecular-level investigation on the interaction of small gas molecules (CO, NO) with Co−TPP and Fe−TPP anchored on a noble metal surface. The following main conclusions can be drawn. (i) With both M−TPP species there is a discriminative response, and the effects of CO vs NO ligation can be clearly distinguished. (ii) The response of Fe−TPP and Co−TPP/Ag(111) to either CO or NO is similar. Either one or two CO ligands can be weakly attached to the functional macrocycle core, whereby the electronic and geometric structure of the surface-confined metalloporphyrin is only marginally influenced. In marked contrast, the observed mononitrosyl coordination strongly affects both the electronic and the geometric structure of the metalloporphyrins. Notably, the HOMO signal is entirely quenched and both a relaxation of the saddle-shape distortion as well as a reduction of the surface−porphyrin interaction are suggested.

This study demonstrates that the bonding of diatomic molecules to functional molecular templates can be monitored in exquisite detail and proves that surface-anchored metalloporphyrin entities may exhibit a behavior different from a solid-state or gas-phase system. Accordingly, the experiments provide interesting opportunities to explore 2D coordination systems with flexible species in a highly controlled environment. We suggest that the findings represent an important step for a thorough understanding of such systems, which open up new avenues to deliberately tune the reactivity of molecular arrays on surfaces for sensing applications or catalytic conversions.

Acknowledgment. This work was supported by the Munich Center for Advanced Photonics (MAP), TUM-IAS, and the ERC Advanced Grant MolArt (#247299). The authors thank Giorgio Zoppellaro and Mario Ruben (INT Karlsruhe) for providing high-purity Co−TPP molecules.

Supporting Information Available: Different imaging modes due to a modified termination of the STM tip; pseudo-3D rendering of CO/Co−TPP topography and dI/dU map. This material is available free of charge via the Internet at http://pubs.acs.org.

JA1054884